

Fluorescence modulation sensing of positively and negatively charged proteins on lipid bilayers

Aaron D Robison, Da Huang, Hyunsook Jung, and Paul S Cremer

Citation: *Biointerphases* **8**, 1 (2013); doi: 10.1186/1559-4106-8-1

View online: <http://dx.doi.org/10.1186/1559-4106-8-1>

View Table of Contents: <http://scitation.aip.org/content/avs/journal/bip/8/1?ver=pdfcov>

Published by the AVS: Science & Technology of Materials, Interfaces, and Processing

Articles you may be interested in

Publisher's Note: "Nanomechanical properties of lipid bilayer: Asymmetric modulation of lateral pressure and surface tension due to protein insertion in one leaflet of a bilayer" [*J. Chem. Phys.* **138**, 065101 (2013)]

J. Chem. Phys. **138**, 139901 (2013); 10.1063/1.4795259

Nanomechanical properties of lipid bilayer: Asymmetric modulation of lateral pressure and surface tension due to protein insertion in one leaflet of a bilayer

J. Chem. Phys. **138**, 065101 (2013); 10.1063/1.4776764

Charging and structure of zwitterionic supported bilayer lipid membranes studied by streaming current measurements, fluorescence microscopy, and attenuated total reflection Fourier transform infrared spectroscopy

Biointerphases **4**, 1 (2009); 10.1116/1.3082042

Polarization-dependent fluorescence of proteins bound to nanopore-confined lipid bilayers

J. Chem. Phys. **129**, 095102 (2008); 10.1063/1.2972143

Forces between charged lipid bilayers: A theoretical model

J. Chem. Phys. **85**, 6010 (1986); 10.1063/1.451515



ORIGINAL ARTICLE

Open Access

Fluorescence modulation sensing of positively and negatively charged proteins on lipid bilayers

Aaron D Robison, Da Huang, Hyunsook Jung and Paul S Cremer*

Abstract

Background: Detecting ligand-receptor binding on cell membrane surfaces is required to understand their function and behavior. Detection platforms can also provide an avenue for the development of medical devices and sensor biotechnology. The use of fluorescence techniques for such purposes is highly desirable as they provide high sensitivity. Herein, we describe a technique that utilizes the sensitivity of fluorescence without directly tagging the analyte of interest to monitor ligand-receptor interactions on supported lipid bilayers. The fluorescence signal is modulated according to the charge state of the target analyte. The binding event elicits protonation or deprotonation of pH-responsive reporter dyes embedded in the lipid bilayer.

Methods: Supported lipid membranes containing *ortho*-conjugated rhodamine B-POPE (1-hexadecanoyl-2-(9Z-octadecenoyl)-*sn*-glycero-3-phosphoethanolamine), which fluoresces in its protonated but not in its deprotonated form, were utilized as sensor platforms for biotin-avidin and biotin-streptavidin binding events. The membranes contained 5 mol% biotin-PE (1,2-dipalmitoyl-*sn*-glycero-3-phosphoethanolamine-*N*-(cap biotiny)) (sodium salt) as a capture ligand. Supported lipid bilayers were formed in the channels of microfluidic devices and the fluorescence intensity of the dye was monitored as protein was introduced.

Results: The binding of avidin, which is positively charged at pH 7.2, made the bilayer surface charge more positive, which in turn deprotonated the *ortho*-rhodamine B dye, reducing its fluorescence. The binding of streptavidin, which is negatively charged at pH 7.2, had the opposite effect. Reducing the ionic strength of the analyte solution by removing 150 mM NaCl from the 10 mM phosphate buffered saline (PBS) solution raised the apparent pKa of the *ortho*-rhodamine B titration point by about 1 pH unit. This could be exploited in conjunction with bulk solution pH changes to turn the rhodamine B-POPE dye into a sensor for streptavidin involving a decrease, rather than an increase, in the fluorescence response, at pH values below streptavidin's pI value.

Conclusions: This study demonstrates the ability to monitor ligand-receptor interactions on supported lipid bilayers through the protonation or deprotonation of reporter dyes for both negatively and positively charged analytes over a range of pH and ionic strength conditions. Specifically, the sensitivity and pH-operating range of this technique can be optimized by modulating the sensing conditions which are employed.

Background

The ability to monitor ligand-receptor interactions is vital for biotechnological advances as well as for a fundamental understanding of cell biology. The single-molecule sensitivity that fluorescent labeling can provide and the relative ease of fluorescence measurements has resulted in the utilization of this technique for detecting and monitoring proteins and nucleotides. Dye labels can, however, interfere with analyte activity and be difficult to efficiently

employ [1,2]. Many sensing techniques have consequently been developed such as quartz-crystal microbalance (QCM), [3-6] surface plasmon resonance (SPR), [7-10] semiconductor nanowire conductivity, [11,12] and optical microcavities that avoid the use of fluorescent labels [13]. Although these techniques avoid the problems associated with directly attaching fluorescent tags to analytes, they can behave non-linearly in response to analyte concentration, require specialized equipment or procedures which can be difficult and/or costly to employ, or possess poorer detection limits than fluorescence-based techniques.

* Correspondence: cremer@mail.chem.tamu.edu
Department of Chemistry, Texas A&M University, 3255 TAMU, College Station, TX 77843, USA

It is advantageous to be able to monitor ligand-receptor interactions on supported lipid bilayers [14] because these platforms effectively act as simplified cellular surfaces, incorporating the same lipid molecules as well as maintaining two-dimensional lipid fluidity [15]. Indeed, the majority of current drug targets are receptor sites associated with the cell surface [16]. This makes the ability to effectively monitor such systems key for therapeutics and drug discovery. Consequently, much work has been done to produce supported lipid bilayers that mimic the cell surface with various supports [17-20] and tethers [21-26]. By embedding these bilayers into microfluidic devices, [27] one can probe binding ligands rapidly while utilizing only small amounts of analyte. Heterogeneous flow-based microfluidic techniques also enable the user to easily modulate parameters such as ionic strength and buffer pH while monitoring the fluorescent response in real time. The ability to utilize glass substrates as membrane supports is also advantageous as these surfaces can readily accommodate fluid lipid bilayers via vesicle fusion [28,29].

Recently, we have developed a sensing technique that employs the sensitivity of fluorescent measurements while avoiding the complications incurred by directly labeling the analyte of interest [30]. This technique involves the incorporation of a pH sensitive dye, *ortho*-conjugated Texas Red DHPE (Texas Red 1,2-dihexadecanoyl-*sn*-glycero-3-phosphoethanolamine, triethylammonium salt), into a supported lipid bilayer. This isomer of Texas Red loses fluorescence when it is deprotonated at higher pH. On the other hand, the *para*-conjugated Texas Red isomer retains its fluorescence under basic conditions and therefore can serve as a reference dye [31]. These Texas Red-containing bilayers can also accommodate binding ligands such as biotin-PE (1,2-dipalmitoyl-*sn*-glycero-3-phosphoethanolamine-*N*-(cap biotinyl) (sodium salt)). Upon the binding of a negatively charged protein, the surface potential near the binding site will be decreased. This helps partition hydronium ions to the interface, which in turn causes protonation of the *ortho*-Texas Red isomer and increases the fluorescence response. This sensing approach, by monitoring the change in fluorescence signal, was demonstrated using the biotin/anti-biotin binding pair [30]. The assay shows sub-pM sensitivity and could be performed with low analyte volumes inside a microfluidic device.

Herein, we have utilized the *ortho* isomer of rhodamine B (Lissamine rhodamine B sulfonyl chloride, mixed isomers) conjugated to the free amine of POPE (1-hexadecanoyl-2-(9Z-octadecenoyl)-*sn*-glycero-3-phosphoethanolamine) as a bilayer-conjugated reporter dye. The *ortho* rhodamine B isomer exhibits much more complete quenching behavior at high pH compared to *ortho*-Texas Red [30,32]. Additionally, the *ortho* isomer of rhodamine B exhibits pH-sensitive fluorescence in a more acidic pH range and is far

less expensive than Texas Red. Significantly, this more acidic dye can be exploited to detect positively charged as well as negatively charged proteins near neutral pH. For positively charged proteins, the sensor works in a manner similar to the detection of negatively charged species, except that a decrease in fluorescence accompanies a binding event because the interfacial potential becomes more positive and the effective local pH is therefore increased. Avidin and streptavidin proteins were employed to test the decreasing and increase fluorescence sensing modalities, respectively (Figure 1), as these proteins demonstrate a high affinity for the same ligand (biotin), but have differing isoelectric points. Avidin has an isoelectric point (pI) of ~10 [33]. It is therefore positively charged at a working pH of 7.2 and, in fact, caused a decrease in the fluorescence response from the bilayer upon protein binding. For streptavidin, there was an increase in the fluorescence upon binding near or above the protein's reported isoelectric point of 6.4 [33]. On the other hand, a decrease in fluorescence accompanied streptavidin binding at pH values below its pI. Finally, by modulating the ionic strength of the buffer employed in this assay, it was possible to both increase sensitivity and shift the apparent pKa of the *ortho*-rhodamine B dye to more basic values.

Methods

Materials

Lissamine rhodamine B sulfonyl chloride was obtained from Invitrogen (Eugene, OR). POPC (1-palmitoyl-2-oleoyl-*sn*-glycero-3-phosphocholine), biotin-PE, and POPE were purchased from Avanti Polar Lipids (Alabaster, AL). The chemical structures of POPC, *ortho*-conjugated rhodamine B-POPE, and biotin-PE are shown in Figure 2. Purified water was obtained from a NANOpure Ultrapure Water System (18.2 M Ω ·cm, Barnstead, Dubuque, IA). Glass coverslips (24 × 40 mm, No. 1.5, Corning Inc.) were used as planar solid supports. PDMS (polydimethylsiloxane, Dow Corning Sylgard Silicone Elastomer-184) was obtained from Krayden, Inc (El Paso, TX). Streptavidin and avidin were purchased from Rockland (Gilbertsville, PA).

Rhodamine B-POPE Conjugation and Separation

A solution of 10 mg of rhodamine B sulfonyl chloride in 1 mL of chloroform was mixed with 10 mg of POPE and 2 μ L of diethylamine. The reaction was stirred for 1 h at room temperature. After the reaction, the solution was spotted onto a TLC plate (EMD, 5715-7, silica gel 60 F254) and developed in a 92:8 mixture by volume of chloroform to methanol to yield separated rhodamine-B labeled POPE isomers. The *ortho*-rhodamine B-POPE isomer was further purified on a second TLC plate developed with an ammonium hydroxide solution, dichloromethane, and *n*-propanol mixture of 5:60:35 by volume. The successful labeling of the phospholipid was confirmed with matrix-

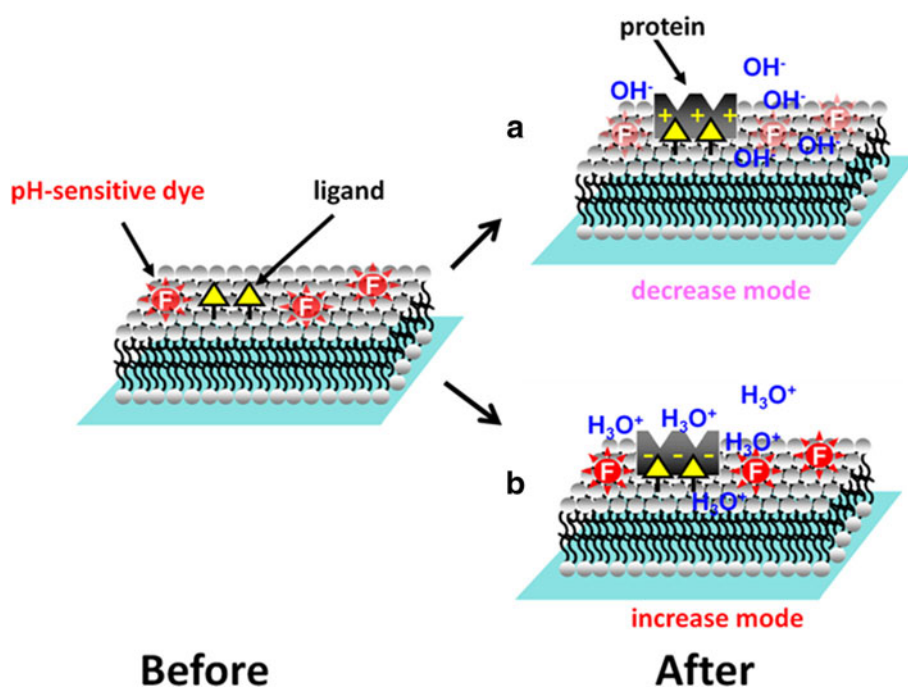


Figure 1 Illustration of the pH modulation assay in detection by either decreasing or increasing the fluorescence response. (a) A positively charged protein (e.g., avidin) recruits hydroxide ions upon binding and renders the membrane surface more basic, decreasing the fluorescence response of the dye. (b) By contrast, a negatively charged protein (e.g., streptavidin) recruits hydronium ions upon surface binding and enhances the fluorescence response of nearby dye molecules.

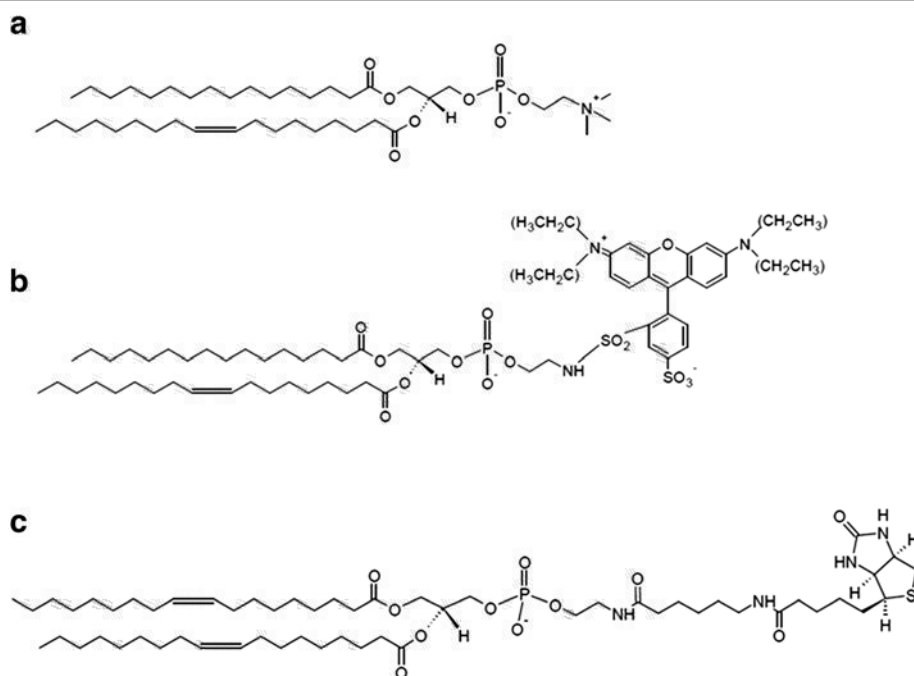


Figure 2 Structures of (a) POPC, (b) POPE-ortho rhodamine B, and (c) biotin-PE.

assisted laser desorption ionization mass spectrometry, which can be seen in Additional file 1: Online Resource 1.

Small Unilamellar Vesicles (SUVs)

To make SUVs, lipids of the desired molar composition were mixed in chloroform and then dried by purging with nitrogen gas. Following desiccation under vacuum for at least 1 h, 0.5 mg/mL lipid suspensions were obtained by hydration with 10 mM phosphate-buffered saline (PBS) containing 150 mM NaCl. The SUV solutions were prepared by ten freeze-thawing cycles with liquid nitrogen and warm water followed by ten extrusion cycles through two stacked 0.1- μ m polycarbonate membranes (Whatman) using a Lipex extruder (Northern Lipids Inc., Vancouver, Canada). The size of the SUVs was determined to be 90 ± 10 nm in diameter by dynamic light scattering (Brookhaven Instruments 90Plus Particle Size Analyzer).

Microfluidic Device Fabrication

Microfluidic devices consisting of a PDMS (polydimethylsiloxane) mold created with a channel-patterned glass substrate were formed by soft lithographic methods [34]. First, photoresist (Shipley 1827) was spin coated onto clean glass slides (soda-lime glass slides, Corning) which were then exposed to UV light through a Kodak technical pan film photomask consisting of the appropriate microfluidic channel pattern. These photoresist-coated glass slides were treated in developing solution and baked overnight at 120°C. The thickness of the photoresist layer was determined to be 2.3 μ m to 2.4 μ m using a Dektak 3 Stylus Profilometer. The patterned glass slides were then etched by immersing them into a buffered oxide etchant (BOE) solution [35]. The BOE solution was prepared by mixing 48% HF (EMD Chemicals Inc., Germany) and aqueous NH_4F (200 g/300 mL purified water, Alfa Aesar, Ward Hill, MA) in a 1:6 volume ratio. The etching process was repeated until the depth of the channels was between 15 μ m and 19 μ m. The slides were then washed with acetone to remove the remaining photoresist and dried under flowing nitrogen gas. Next, PDMS (Sylgard silicone elastomer-184) and its cross-linking agent (10:1 volume ratio) were mixed in a plastic beaker and degassed inside a desiccator under vacuum. The liquid PDMS mixture was poured over a patterned glass slide and allowed to cure in an oven at 70°C. After 1 h, the nascently-formed PDMS elastomer was peeled off of the glass slide. This mold and a freshly cleaned glass coverslip were placed into a 25 W oxygen plasma cleaner (PDC-32 G, Harrick) for 30 s and were then immediately brought into contact to form the PDMS/glass microfluidic device. It should be noted that both the glass slides and coverslips used in these procedures were cleaned in a boiling solution of ICN 7X

detergent (Costa Mesa, CA) mixed with purified water at a 1:4 volume ratio. Following this, the slides were annealed in a kiln (Sentry Xpress 2.0, Orton Ceramic Foundation, OH) at 500°C for 5 h before the oxygen plasma treatment.

Supported Lipid Bilayers (SLBs)

SLBs were formed within the channels of microfluidic devices via spontaneous vesicle fusion [28]. Five μ L of an SUV solution was injected into each microchannel and incubated for 10 min followed by rinsing with pure PBS buffer to remove excess vesicles. For protein detection measurements, solutions of either avidin or streptavidin were continually flowed through each channel for up to 1 h.

pH Titration of SLBs

PBS solutions with and without 150 mM NaCl were prepared at pH values ranging from 4.5 to 10.5 by mixing with appropriate amounts of Na_2HPO_4 , NaH_2PO_4 , or Na_3PO_4 . The pH was measured with a standard glass electrode setup having an absolute error of ± 0.1 pH units. Titration curves of the fluorescence from the dye molecules in the SLBs were obtained by systematically changing the pH of the bulk solution by flowing the appropriate pH adjusted buffer solutions through the microfluidic device in a stepwise fashion. The value of the pH for each buffer was determined immediately prior to adding it to the microfluidic channels.

Fluorescence Microscopy

All fluorescence images were obtained using a Nikon Eclipse Ti-U fluorescence microscope (Tokyo, Japan) equipped with a ProEM 1024 CCD camera (Princeton Instruments). A 10 \times air objective (N.A. = 0.45) was used for all detection measurements. The light source was a Lumen 200 (Prior Scientific) and a Texas Red filter set (Chroma Technology, Bellows Falls, VT) was employed. All images were processed with MetaMorph software (Version 7.7.0.0, Universal Imaging).

Results and discussion

pH Titration Curves

Initial experiments were performed to obtain titration curves for 0.5 mol% *ortho*-rhodamine B-POPE in POPC bilayers with 0 and 5 mol% biotin PE (Figure 3). The pH of the bulk solution above the bilayers was altered via the continuous flow of pH adjusted 10 mM PBS solutions with 150 mM NaCl. The fluorescence was monitored until a steady state was reached. Once the fluorescent intensity stabilized at a given pH, the value was recorded and a different pH solution was flowed over the bilayer. Representative intensity line scans after reaching steady state can be found in Figure 3a. The bilayer fluorescence data were

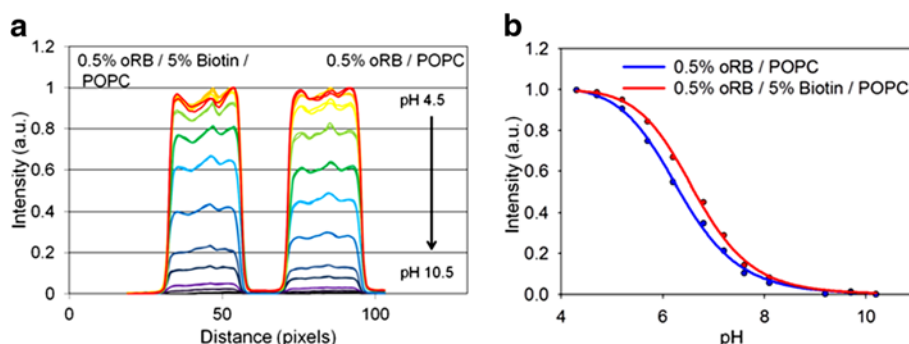


Figure 3 pH titration: (a) Fluorescence intensity line scans across channels containing bilayers composed of 0.5 mol% *ortho*-rhodamine B POPE (oRB) in POPC with and without 5 mol% biotin-PE. (b) Titration curves for each membrane composition. The y-axis values were obtained by dividing the intensity of the fluorescence line scan at each pH value by the maximum fluorescence intensity line scan at pH 4.5. The solid circles represent individual fluorescence measurements and the solid lines are sigmoidal fits to the data.

normalized to the pH value with the maximum fluorescence intensity. Fluorescence intensity measurements versus pH value curves for the two bilayer conditions were fit to a sigmoidal curve (solid lines in Figure 3b) and the apparent pKa values were 6.2 ± 0.1 and 6.5 ± 0.1 , respectively, for bilayers with 0 mol% and 5 mol% biotin-PE.

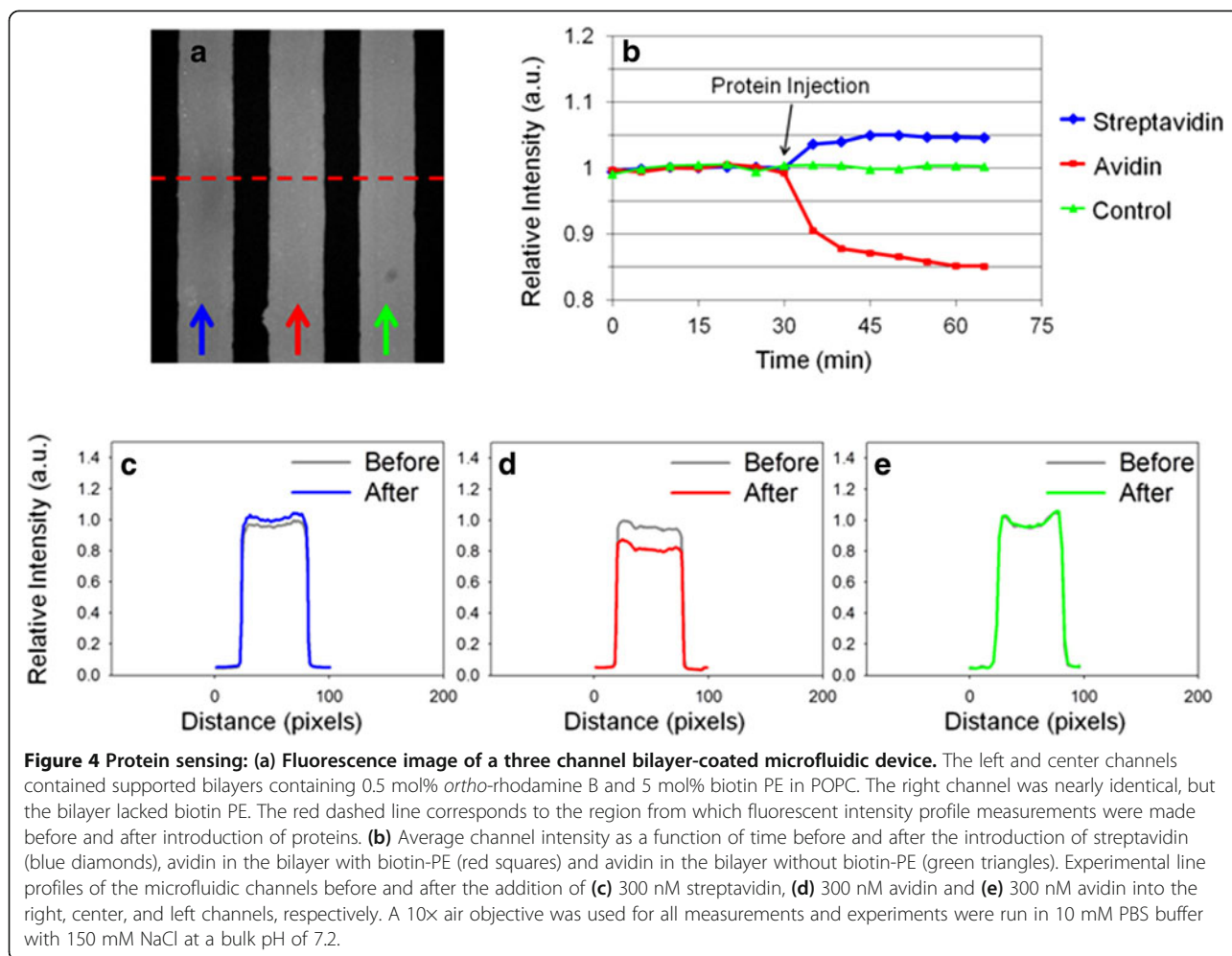
Sensing Avidin and Streptavidin

Next, experiments were performed with POPC bilayers containing 5 mol% biotin PE and 0.5 mol% *ortho*-rhodamine B POPE in both fluorescence increasing and fluorescence decreasing assays. For these experiments, avidin and streptavidin were utilized as the binding analytes of interest. In fact, both proteins have a strong affinity for biotin [36]. Experiments were performed at pH 7.2, which falls within the linear response range of the dye as a function of pH (Figure 3). Under these conditions, streptavidin carries a net negative charge while avidin carries a net positive charge [33]. Experiments were run in three parallel microfluidic channels. Supported POPC bilayers containing *ortho*-rhodamine B-POPE and biotin PE were present in the first two channels. In the third channel, a control POPC bilayer was employed which contained *ortho*-rhodamine B-POPE, but no biotin PE (Figure 4a). Fluorescent micrographs were captured every five minutes as 10 mM PBS buffer at pH 7.2 with 150 mM NaCl was flowed through the channels until fluorescence stabilization was achieved. Next, 300 nM of streptavidin was introduced into left channel, while 300 nM of avidin was flowed into the middle and right channels (30 min. mark). Data were collected every five minutes and the fluorescence intensity data came to equilibrium within an hour after introducing the protein. The fluorescence intensity values from each channel as a function of time are shown in Figure 4b. Moreover, the individual fluorescence line scans at 0 and 65 minute marks are shown in

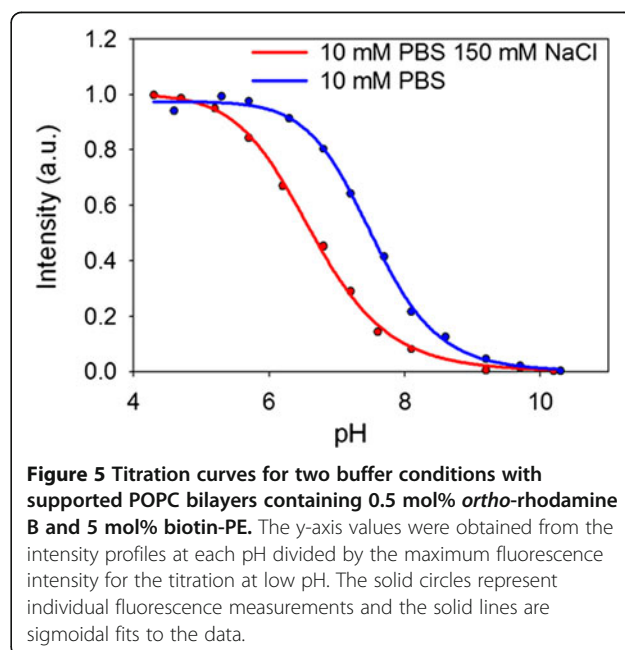
Figures 4c-e. As can be seen, the introduction of streptavidin into the left channel caused the fluorescence to increase by about 5%. On the other hand, the addition of avidin into the middle channel resulted in a decrease in fluorescence intensity by about 20%. The control channel (on the right in the image) showed no change in signal upon the addition of avidin. An additional control experiment using streptavidin in the absence of biotin-PE ligands also showed no change in fluorescence (Additional file 1: Online Resource 2). The difference in fluorescence changes elicited by streptavidin and avidin reflects the isoelectric point of each protein at the operating pH of the assay. Indeed, the experiments were conducted just above the isoelectric point for streptavidin, but far below the isoelectric point for avidin. Consequently, avidin should be more highly charged under these conditions [37] and therefore should perturb the apparent local pH above the supported lipid bilayer to a greater extent upon binding. Finally, it was necessary to ensure that the decreasing fluorescence intensity assay for avidin was indeed due to a decrease in the local hydronium ion concentration caused by protein binding rather than mere photobleaching of the dye. To check this, control experiments were carried out on biotinylated membranes utilizing the pH-insensitive *para* isomer of rhodamine B-labeled POPE with 5 mol% biotin-PE. As expected, the fluorescence intensity did not change in this assay (Additional file 1: Online Resource 3).

Altering Buffer Conditions to Optimize Assay Design

To probe the effect of salt screening on fluorescence response, experiments were carried out using 10 mM PBS without NaCl. This resulted in a buffer with decreased ionic strength and consequentially an increased Debye length [38]. This should enhance the sensitivity of the assay by increasing the area of the



bilayer that will be influenced by the binding of a protein. Specifically, under high salt conditions (150 mM NaCl) in a 10 mM PBS buffer, the Debye length should be about 6.6 Å [38]. On the other hand, when the 10 mM PBS buffer is used without NaCl, the Debye length is about 12.4 Å. Thus decreasing the salt concentration allows each surface-bound protein to influence a greater range of dye molecules in its proximity. Titration curves performed under low and high salt concentrations were performed (Figure 5). These experiments were run in the absence of protein molecules in bilayers consisting of 0.5 mol% *ortho*-rhodamine B and 5 mol% biotin-PE in POPC. As can be seen, the low salt concentration conditions resulted in a shift in the apparent pKa of the *ortho*-rhodamine B dye by about 1 pH unit (the line scans from which these titration curves were created can be seen in Additional file 1: Online Resource 4). This shift is not surprising considering that decreasing the ionic strength of a solution should increase the apparent pKa of a titratable species as predicted by Debye-Hückel theory [39]. As a consequence of lowering the salt concentration, the linear pH responsive range of



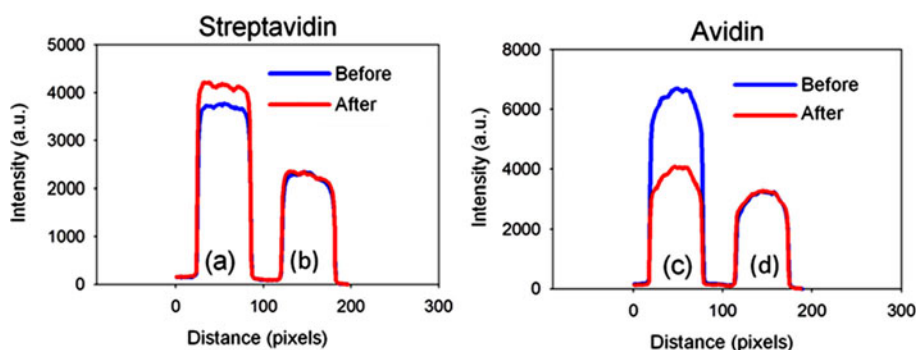


Figure 6 Protein sensing in 10 mM PBS: Line scans for microfluidic channels before and after the introduction of (left) streptavidin and (right) avidin. (a) A supported bilayer composed of 0.5 mol% *ortho*-rhodamine B and 5 mol% biotin-PE in POPC before and after the addition of streptavidin (blue and red, respectively). (b) A control bilayer composed of 0.5 mol% *ortho*-rhodamine B in POPC before and after addition of streptavidin. (c) A bilayer composed of 0.5 mol% *ortho*-rhodamine B and 5 mol% biotin-PE in POPC before and after the addition of avidin, and (d) a control bilayer composed of 0.5 mol% *ortho*-rhodamine B in POPC before and after the addition of avidin.

the assay is shifted to a higher value. In fact, this allows the assay to be run at pH 8.1, where streptavidin is more negatively charged, but avidin is somewhat less positively charged as described below.

To test the effects of the low ionic strength conditions on sensor response, bilayers were formed inside two parallel microfluidic channels with and without 5 mol% biotin-PE. The bilayers were rinsed with 10 mM PBS until the fluorescence stabilized. Next, 300 nM streptavidin was introduced above the supported bilayers in a pH 8.1 buffer composed of 10 mM PBS and 150 mM NaCl and flowed for 30 minutes until the fluorescence response stabilized. Finally, the channels were flushed with 10 mM PBS buffer until the signal stabilized again. Identical experiments were also performed with avidin. As can be seen in Figure 6, the introduction of streptavidin resulted in an increase in fluorescence whereas the introduction of avidin resulted in a fluorescence decrease just as in Figure 4; however, the relative signal changes were greater (Table 1).

As can be seen from Table 1, the results from the low ionic strength experiments were remarkable. In fact, the percentage change in fluorescence upon the introduction of streptavidin was approximately a factor of three greater than when 150 mM NaCl was present. The change for avidin was even larger, a factor of six. This is

somewhat curious, as avidin should contain a smaller charge at pH 8.1 compared with 7.2, as it is closer to its isoelectric point. As such, the relatively large change in signal for avidin must be dominated by the increase in the Debye length under these conditions.

To explore the role of the assay's pH relative to the pI value of a protein analyte, a final set of experiments was designed in which the fluorescence response was monitored as a function of pH at constant ionic strength for streptavidin. Because the isoelectric point for this protein is just below neutral pH, [33] it is expected that the assay should switch from an increased fluorescence response to decreased response when the experiments are run at 5.9 instead of 7.3. To test this idea, supported POPC bilayers were formed with 0.5 mol% *ortho*-rhodamine B and 5 mol% biotin-PE in two parallel microfluidic channels. In each case, the solution contained 10 mM PBS with 150 mM NaCl. The normalized fluorescence intensity from these channels are provided in Figure 7. For the first 20 minutes of each run, pure

Table 1 Summary of protein signal changes for various experimental conditions

| Protein (300 nM) | 10 mM PBS Buffer Conditions | Average % Change in Signal upon Protein Binding |
|------------------|-----------------------------|---|
| Streptavidin | pH 7.2 w/ 150 mM NaCl | +7 |
| | pH 8.1 | +21 |
| | pH 5.9 w/ 150 mM NaCl | -5 |
| Avidin | pH 7.2 w/ 150 mM NaCl | -12 |
| | pH 8.1 | -74 |

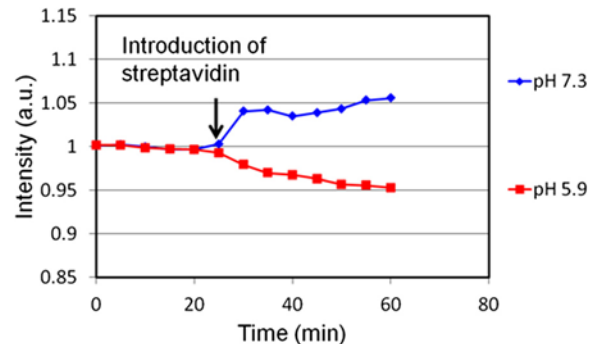


Figure 7 Fluorescence intensity measurements before and after the addition of streptavidin to buffers at pH 7.3 and 5.9. Both buffers contained 10 mM PBS and 150 mM NaCl. Each point represents the average fluorescence intensity inside the microfluidic channels as a function of time.

buffer at a given pH was flowed over the bilayer. This provided a fluorescence intensity benchmark with which to compare protein-bound conditions. Following stabilization, 300 nM streptavidin was introduced into the respective rinsing buffers and monitored. As can be seen, a fluorescence intensity increase was found at pH 7.3, but pH 5.9 showed a decrease. The latter result is consistent with the idea that the protein is below its pI of 6.4 [33].

Conclusions

Two important considerations needed to be taken into account when employing the pH modulation sensor described herein. First, it is necessary to operate this assay in a pH window where the fluorescence response can be modulated. Second, it is important that proteins of interest be tested sufficiently far away from their pI values to elicit a fluorescence response. Through manipulation of the ionic strength of the operating buffer, it is possible to widen the assay range in order to accommodate proteins with a variety of different pI values. However, it should also be noted that the surface chemistry of the membrane and the underlying solid support play an important role in determining the surface potential. These variables too could be modulated by changing the substrate type or specific lipid membrane chemistry. Additional file 1: Online Resource 5 demonstrates that the addition of charged lipids to the membrane, the addition of osmolytes to the buffer, or even changing the nature of the buffer ions can all affect the titration curve for the dye. Of course, modifications to the dye itself would also change the range in which the assay can be operated.

Although numerous variables can be manipulated to change the operating range of the assay, it should be noted that changing these variables may also modulate the detection limits of this assay. Such behavior could be quite complex. Indeed, in the case of avidin, running the assay at lower ionic strength, but higher pH, (8.1 instead of 7.3) resulted in a greater signal response despite the fact that the protein was actually closer to its isoelectric point (Figure 6). In this particular case, the lower ionic strength was the determining factor. Moreover, it could also be shown that decreasing the ionic strength of the buffer at constant pH increased the sensitivity for streptavidin detection (Additional file 1: Online Resource 6). Further studies will be required to determine if other variables such as analyte charge density or specific chemistry can be the determining factors in fluorescence changes. Such studies are now being undertaken.

This pH modulation sensor represents a facile and rapid method for detecting binding events on supported lipid bilayers. As such, it may serve as a screen for monitoring protein-ligand interactions in biophysical assays of membranes. Further quantification of this technique

should be possible by exploiting QCM-D [3-6] or SPR [7-10] as complementary approaches to help determine the number density of analyte proteins and perhaps even the charge per analyte. Moreover, complementary techniques may also help quantify potential interference effects and related platform biofouling effects when more complex, real-world biological samples are analyzed.

Additional file

Additional file 1: Online Resource 1: Matrix assisted laser desorption ionization mass spectrum showing a peak at 1258.6 for rhodamine-B POPE + 2H⁺. Online Resource 2: Fluorescence intensity line profile data corresponding to a bilayer composed of 0.5 mol% *ortho*-rhodamine B-POPE in POPC before and after the addition of 300 nM streptavidin. The assay was run with 10 mM PBS with 150 mM NaCl at pH 7.2. **Online Resource 3:** Fluorescence intensity line profile data corresponding to a bilayer composed of 5 mol% biotin and 0.5 mol% *para*-rhodamine B-POPE in POPC before and after the addition of 300 nM avidin. The assay was run with 10 mM PBS with 150 mM NaCl at pH 7.2. **Online Resource 4:** Fluorescence intensity line profile data from which titration curves were extracted in (Figure 5). **Online Resource 5:** Representative titration curves for various buffers and bilayer chemistries. NaOH and HCl were used to modulate the pH with each buffer used. **Online Resource 6:** Fluorescence response relative to a normalized starting intensity of 1.00 for the addition of 300 nM streptavidin at pH 8.1 in buffers of varying ionic strength. The assays were run with POPC bilayers containing 0.5 mol% *ortho*-rhodamine B-POPE and 5 mol% biotin-PE. The error bars correspond to the standard deviation of three fluorescent measurements.

Competing interests

Texas A&M University and Phluorescent Technology have patent applications pending covering pH modulation assays and *ortho*-rhodamine B conjugated lipids. PSC, DH, and ADR were the coauthors of these applications and have an interest in Phluorescent Technology.

Authors' contributions

ADR conducted the protein-sensing experiments, while DH synthesized and separated reporter fluorescent dyes. HJ conducted preliminary protein sensing experiments. ADR and PSC prepared the manuscript. PSC also served as Principle Investigator and coordinated all research. All authors read and approved the final manuscript.

Acknowledgment

This work was funded by the Office of Naval Research (N00014-08-1-0467).

Received: 6 December 2012 Accepted: 17 January 2013

Published: 17 January 2013

References

1. Kodadek T (2001) Protein microarrays: prospects and problems. *Chem Biol* 8(2):105-115
2. Yu XB, Xu DK, Cheng Q (2006) Label-free detection methods for protein microarrays. *Proteomics* 6(20):5493-5503. doi:10.1002/pmic.200600216
3. Cooper MA, Dultsev FN, Minson T, Ostanin VP, Abell C, Klenerman D (2001) Direct and sensitive detection of a human virus by rupture event scanning. *Nat Biotechnol* 19(9):833-837
4. Furusawa H, Komatsu M, Okahata Y (2009) In situ monitoring of conformational changes of and peptide bindings to calmodulin on a 27 MHz quartz-crystal microbalance. *Anal Chem* 81(5):1841-1847. doi:10.1021/Ac8022229
5. Muratsugu M, Ohta F, Miya Y, Hosokawa T, Kurosawa S, Kamo N, Ikeda H (1993) Quartz-crystal microbalance for the detection of microgram quantities of human serum-albumin - relationship between the frequency change and the mass of protein adsorbed. *Anal Chem* 65(20):2933-2937
6. Cooper MA, Singleton VT (2007) A survey of the 2001 to 2005 quartz crystal microbalance biosensor literature: applications of acoustic physics to the

- analysis of biomolecular interactions. *J Mol Recognit* 20(3):154–184. doi:10.1002/Jmr.826
7. Yang CY, Brooks E, Li Y, Denny P, Ho CM, Qi FX, Shi WY, Wolinsky L, Wu B, Wong DTW, Montemagno CD (2005) Detection of picomolar levels of interleukin-8 in human saliva by SPR. *Lab Chip* 5(10):1017–1023. doi:10.1039/B504737d
 8. Anker JN, Hall WP, Lambert MP, Velasco PT, Mrksich M, Klein WL, Van Duyne RP (2009) Detection and identification of bioanalytes with high resolution LSPR spectroscopy and MALDI mass spectrometry. *J Phys Chem C* 113(15):5891–5894. doi:10.1021/Jp900266k
 9. Das A, Zhao J, Schatz GC, Sligar SG, Van Duyne RP (2009) Screening of type I and II drug binding to human cytochrome P450-3A4 in nanodiscs by localized surface plasmon resonance spectroscopy. *Anal Chem* 81(10):3754–3759. doi:10.1021/Ac802612z
 10. Wegner GJ, Lee HJ, Corn RM (2002) Characterization and optimization of peptide arrays for the study of epitope-antibody interactions using surface plasmon resonance imaging. *Anal Chem* 74(20):5161–5168. doi:10.1021/Ac025922u
 11. Wang WU, Chen C, Lin KH, Fang Y, Lieber CM (2005) Label-free detection of small-molecule-protein interactions by using nanowire nanosensors. *P Natl Acad Sci USA* 102(9):3208–3212. doi:10.1073/pnas.0406368102
 12. Patolsky F, Zheng GF, Lieber CM (2006) Nanowire-based biosensors. *Anal Chem* 78(13):4260–4269
 13. Armani AM, Kulkarni RP, Fraser SE, Flagan RC, Vahala KJ (2007) Label-free, single-molecule detection with optical microcavities. *Science* 317(5839):783–787. doi:10.1126/science.1145002
 14. Tamm LK, McConnell HM (1985) Supported phospholipid-bilayers. *Biophys J* 47(1):105–113
 15. Cremer PS, Boxer SG (1999) Formation and spreading of lipid bilayers on planar glass supports. *J Phys Chem B* 103(13):2554–2559
 16. Christopoulos A (2002) Allosteric binding sites on cell-surface receptors: novel targets for drug discovery. *Nat Rev Drug Discov* 1(3):198–210. doi:10.1038/Nrd746
 17. Yi F, Xu J, Smith AM, Parikh AN, Lavan DA (2009) Nanofiber-supported phospholipid bilayers. *Soft Matter* 5(24):5037–5041. doi:10.1039/B903048d
 18. Shen SK, Kendall E, Oliver A, Ngassam V, Hu DD, Parikh AN (2011) Liposil-supported lipid bilayers as a hybrid platform for drug delivery. *Soft Matter* 7(3):1001–1005. doi:10.1039/C0sm00730g
 19. Ma C, Srinivasan MP, Waring AJ, Lehrer RI, Longo ML, Stroeve P (2003) Supported lipid bilayers lifted from the substrate by layer-by-layer polyelectrolyte cushions on self-assembled monolayers. *Colloid Surface B* 28(4):319–329
 20. Diaz AJ, Albertorio F, Daniel S, Cremer PS (2008) Double cushions preserve transmembrane protein mobility in supported bilayer systems. *Langmuir* 24(13):6820–6826. doi:10.1021/La800018d
 21. Wagner ML, Tamm LK (2000) Tethered polymer-supported planar lipid bilayers for reconstitution of integral membrane proteins: silane-polyethyleneglycol-lipid as a cushion and covalent linker. *Biophys J* 79(3):1400–1414
 22. Giess F, Friedrich MG, Heberle J, Naumann RL, Knoll W (2004) The protein-tethered lipid bilayer: a novel mimic of the biological membrane. *Biophys J* 87(5):3213–3220. doi:10.1529/biophysj.104.046169
 23. Atanasov V, Knorr N, Duran RS, Ingebrandt S, Offenhausser A, Knoll W, Koper I (2005) Membrane on a chip: a functional tethered lipid bilayer membrane on silicon oxide surfaces. *Biophys J* 89(3):1780–1788. doi:10.1529/biophysj.105.061374
 24. Taylor JD, Linman MJ, Wilkop T, Cheng Q (2009) Regenerable tethered bilayer lipid membrane arrays for multiplexed label-free analysis of lipid-protein interactions on poly(dimethylsiloxane) microchips using SPR imaging. *Anal Chem* 81(3):1146–1153. doi:10.1021/Ac8023137
 25. Han XJ, Achalkumar AS, Bushby RJ, Evans SD (2009) A cholesterol-based tether for creating photopatterned lipid membrane arrays on both a silica and gold surface. *Chem-Eur J* 15(26):6363–6370. doi:10.1002/chem.200900404
 26. Junghans A, Champagne C, Cayot P, Loupiac C, Koper I (2011) Probing protein-membrane interactions using solid supported membranes. *Langmuir* 27(6):2709–2716. doi:10.1021/La103200k
 27. Yang TL, Jung SY, Mao HB, Cremer PS (2001) Fabrication of phospholipid bilayer-coated microchannels for on-chip immunoassays. *Anal Chem* 73(2):165–169
 28. Brian AA, McConnell HM (1984) Allogeneic stimulation of cyto-toxic T-cells by supported planar membranes. *P Natl Acad Sci-Biol* 81(19):6159–6163
 29. McConnell HM, Watts TH, Weis RM, Brian AA (1986) Supported planar membranes in studies of cell-cell recognition in the immune-system. *Biochim Biophys Acta* 864(1):95–106
 30. Jung H, Robison AD, Cremer PS (2009) Detecting protein-ligand binding on supported bilayers by local pH modulation. *J Am Chem Soc* 131(3):1006–1014. doi:10.1021/Ja804542p
 31. Corrie JET, Davis CT, Eccleston JF (2001) Chemistry of sulforhodamine-amine conjugates. *Bioconjugate Chem* 12(2):186–194
 32. Corrie JET, Eccleston JF, Ferenczi MA, Moore MH, Turkenburg JP, Trentham DR (2008) Ring-chain interconversion of sulforhodamine-amine conjugates involves an unusually labile C-N bond and allows measurement of sulfonamide ionization kinetics. *J Phys Org Chem* 21(4):286–298. doi:10.1002/Poc.1318
 33. Skander M, Humbert N, Collet J, Gradinaru J, Klein G, Loosli A, Sauser J, Zocchi A, Gilardoni F, Ward TR (2004) Artificial metalloenzymes: (Strept) avidin as host for enantioselective hydrogenation by achiral biotinylated rhodium-diphosphine complexes. *J Am Chem Soc* 126(44):14411–14418. doi:10.1021/Ja0475718
 34. Xia YN, McClelland JJ, Gupta R, Qin D, Zhao XM, Sohn LL, Celotta RJ, Whitesides GM (1997) Replica molding using polymeric materials: a practical step toward nanomanufacturing. *Adv Mater* 9(2):147–149
 35. Holden MA, Kumar S, Castellana ET, Beskok A, Cremer PS (2003) Generating fixed concentration arrays in a microfluidic device. *Sensor Actuat B-Chem* 92(1–2):199–207. doi:10.1016/S0925-4005(03)00129-1
 36. Green NM (1990) Avidin and streptavidin. *Method Enzymol* 184:51–67
 37. Monson CF, Pace HP, Liu CM, Cremer PS (2011) Supported bilayer electrophoresis under controlled buffer conditions. *Anal Chem* 83(6):2090–2096. doi:10.1021/Ac1028819
 38. Israelachvili JN (2011) *Intermolecular and Surface Forces*, 3rd edn. Academic Press, San Diego
 39. Metzler DE, Metzler CM (2001) *Biochemistry: The Chemical Reactions of Living Cells*. vol v. 1. Harcourt/Academic Press, San Diego

doi:10.1186/1559-4106-8-1

Cite this article as: Robison et al.: Fluorescence modulation sensing of positively and negatively charged proteins on lipid bilayers. *Biointerphases* 2013 **8**:1.

Submit your manuscript to a SpringerOpen® journal and benefit from:

- Convenient online submission
- Rigorous peer review
- Immediate publication on acceptance
- Open access: articles freely available online
- High visibility within the field
- Retaining the copyright to your article

Submit your next manuscript at ► springeropen.com